Differentiator-based velocity observer with sensor bias estimation: an inverted pendulum case study

Igor Ryadchikov, Stanislav Aranovskiy, Evgeny Nikulchev, Jian Wang, Dmitry Sokolov

Differentiator-based velocity observer with sensor bias estimation: an inverted pendulum case study [⋆]

Igor Ryadchikov [*] **Stanislav Aranovskiy** [**]
Evgeny Nikulchev [***] **Jian Wang** [****] **Dmitry Sokolov** [†]

[*] *Kuban State University, Krasnodar, Russia*
[**] *Equipe Automatique, CentaleSupélec — IETR, Cesson-Sévigné, France; (email: stanislav.aranovskiy@centralesupelec.fr)*
[***] *MIREA — Russian Technological University, Moscow, Russia*
[****] *School of Automation, Hangzhou Dianzi University, Xiasha Higher Education Zone, Hangzhou, Zhejiang, PR China*
[†] *Université de Lorraine, CNRS, Inria, LORIA, F-54000 Nancy, France*

Abstract: In this paper we consider the problem of velocity estimation and stabilization for balancing an inverted pendulum equipped with a reaction wheel. A homogeneous differentiator is proposed for velocity estimation, and it is shown that a bias in sensor readings yields steady-state estimation error. The proposed observer is augmented with a reduced-order bias estimator and local asymptotic stability of the coupled observers is shown. The proposed solution is tested and compared with another approach on an experimental setup.

Keywords: Velocity observer, differentiator, sensor bias, inverted pendulum, reaction wheel

1. INTRODUCTION

This research is motivated by the walking robot with a non-anthropomorphic dynamic stabilization system that we have recently reported in Ryadchikov et al. (2018). For this robot, the idea was to provide auxiliary means of vertical stabilization by installing inside the robot's body two flywheels (shown in red in the Figure 1, left), improving vertical stability without affecting the rest of the mechanical system. The flywheels are orthogonal to each other and the problem of vertical stabilization of the robot can be considered for each axis separately. Thus, we consider a stabilization of a one-dimensional reaction-wheel based inverted pendulum as a basic approximation for the robot motion control system.

Inverted pendulums, including reaction-wheel setups, have been extensively studied. Spong et al. (2001) proposed a switching controller to swing the pendulum upwards from its downright equilibrium. The monograph Block et al. (2007) deeply covers the pendulum motion, including linear and nonlinear models, and models of the sensors and actuators that are used for feedback control. Finally, for our paper, the most relevant work is the Cubli by Gajamohan et al. (2012), a very interesting project created at ETH Zürich.

The key element for the stabilization of an inverted pendulum is velocity estimation both for the pendulum and for the reaction wheel. While in the Cubli device, a gyroscope sensor is used to measure the velocity, in our case we use optical angular encoders, and the velocities are to be estimated from the available measurements. Velocity (or momenta) observer design for a mechanical system is a well-known and long-standing problem, see, for example, the recent work by Aranovskiy et al. (2017) where several solutions are considered and compared. While nonlinear Luenberger-like observers and Kalman-based filters operate with the whole vector of measurements and can be computationally demanding, a common engineering approach is to consider each degree of freedom separately and estimate velocity as a derivative of a scalar position (angle) signal; in such a case velocity estimation is considered as a differentiator design problem. There are multiple known solutions for numerical differentiation, such as linear approximation based on Taylor series expansion, *e.g.* a first-order difference used by Spong et al. (2001), sliding-mode exact differentiators first proposed by Levant (1998), or high-gain differentiators as described by Vasiljevic and Khalil (2008). For this paper, we are particularly interested in the homogeneous differentiator (HOMD) proposed by Perruquetti et al. (2008) that ensures finite-time con-

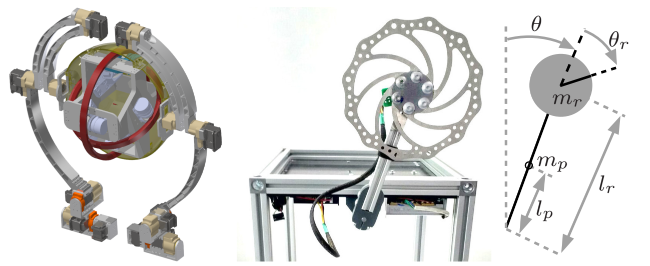

Fig. 1. **Left:** AnyWalker robot uses reaction wheels (shown in red) as an auxiliary stabilization system. **Middle and right:** 1D pendulum hardware and corresponding notations.

[⋆] This work was supported by the Russian Ministry of Education and Science, through the grant No. 8.2321.2017.

vergence and is robust with respect to possible model uncertainties.

An important issue for pendulum stabilization is a sensor bias potentially present in the position measures. This bias can be caused by imprecisions in sensor placement; however, there are other possible sources. For example, in the one-dimensional prototype considered in this paper the motor cable creates a disturbance that shifts the equilibrium point from zero readings of the position sensor. As it is shown by Block et al. (2007) and illustrated in §4, such a bias may shift the stable equilibrium of the closed-loop system away from the origin, that is undesirable behavior for robot stabilization. Thus, the bias should be estimated and taken into account by the control design. Unfortunately, differentiator-based observers cannot be used here since the bias is not a derivative of any measured signal. One possible solution is to use an extended full-state observer instead of differentiators. Another solution was used in the Cubli project by Gajamohan et al. (2012), where the sensor offset was estimated at a slower time scale from the observed equilibrium, see §6 for more details.

In this paper, we propose a novel solution. More precisely, a contribution of this paper is twofold. First, we design a finite-time HOMD-based velocity observer for a reaction-wheel inverted pendulum and use this observer for pendulum stabilization. Second, we propose to combine this observer with a reduced-order sensor bias estimator. Our analysis shows that the resulting coupled nonlinear observer does not preserve the finite-time convergence property, however, under a proper choice of tuning gains the coupled system is locally asymptotically stable and estimation errors converge to zero with a certain domain of attraction. Moreover, it is also shown that the gains can be tuned by the means of linear matrix inequalities (LMIs). The proposed solution is implemented in an experimental setup and compared with the solution proposed by Gajamohan et al. (2012).

The rest of the paper is organized as follows. In §2 we present a model of the considered system and a stabilizing LQR control. Next, in §3 we design HOMD-based observers to estimate pendulum and reaction wheel velocities. The behavior of the closed-loop system with biased measurements is analyzed in §4 and a reduced-order bias observer is proposed and analyzed in §5. Finally, experimental results and comparison with the bias observer used for the Cubli project are given in §6.

2. PENDULUM MODEL AND LQR CONTROL

Model description and used notations. In this section we follow the notations from Block et al. (2007): our main variables are θ and θ_r, where θ is the angle between the pendulum and the vertical, and θ_r is the angle of the reaction wheel w.r.t the pendulum. Refer to Figure 1 for an illustration; Table 1 provides all necessary measurements and notations used in the paper.

Neglecting the friction, we derive the equations of motion (the derivations are based on standard arguments for mechanical systems and are omitted here due to the lack of space):

Table 1. Parameters of the experimental setup.

Description	Symbol	Value
Mass of the pendulum, kg	m_p	0.58
Pivot – pendulum's center of mass distance, m	l_p	0.10
Moment of inertia of the pendulum around its center of mass, kg·m^2	J_p	$3.8{\cdot}10^{-3}$
Mass of the reaction wheel, kg	m_r	0.35
Pivot – reaction wheel axis distance, m	l_r	0.22
Moment of inertia of the reaction wheel, kg·m^2	J_r	$12.48 \cdot 10^{-4}$
Current-to-torque gain, N/A	k	$3.69 \cdot 10^{-2}$
Sampling frequency, Hz	–	500
Resolution of the reaction wheel angle measurement, rad	–	$6.54{\cdot}10^{-2}$
Resolution of the pendulum angle measurement, rad	–	$6.28{\cdot}10^{-4}$

$$\begin{aligned} J_r\ddot{\theta}_r + J_r\ddot{\theta} &= kI, \\ (J+J_r)\ddot{\theta} + J_r\ddot{\theta}_r &= mlg\sin\theta, \end{aligned} \tag{1}$$

where the symbols are as defined in Table 1, $ml := m_pl_p + m_rl_r$, $J := J_p + m_pl_p^2 + m_rl_r^2$, and I is the current in the motor windings. Assuming an internal fast-time-scale current loop, we consider I as our input control signal.

The control goal is to locally stabilize the pendulum in the upper equilibrium, that is to drive the variables θ, $\dot{\theta}$, and $\dot{\theta}_r$ to zero, while $\theta_r \in \mathbb{R}$. Let us further denote the upper equilibrium as the set $\Omega_0 := \left\{\theta = \dot{\theta} = \dot{\theta}_r = 0,\ \theta_r \in \mathbb{R}\right\} \subset \mathbb{R}^4$, which is an invariant set of the system (1). In what follows we say that a control law (locally) stabilizes the system (1) if under this control law the set Ω_0 is (locally) attractive.

Define the state variable vector $x := \begin{bmatrix}\theta\ \dot{\theta}\ \dot{\theta}_r\end{bmatrix}^\top$. Then the control goal is to construct the control input I such that the state x locally converges to the origin.

LQR control design. To achieve the goal, the model (1) is linearized around the equilibrium $x_{eq} := [0\ 0\ 0]^\top$ yielding the linearized model

$$\dot{x} = Ax + BI, \quad \theta = Cx, \tag{2}$$

where θ is the measured output and

$$A := \begin{bmatrix} 0 & 1 & 0 \\ \frac{mlg}{J} & 0 & 0 \\ -\frac{mlg}{J} & 0 & 0 \end{bmatrix}, \quad B := \begin{bmatrix} 0 \\ -\frac{k}{J} \\ \frac{(J+J_r)k}{J\,J_r} \end{bmatrix}, \quad C := \begin{bmatrix} 1 \\ 0 \\ 0 \end{bmatrix}^\top.$$

To stabilize the pendulum the LQR is designed:

$$u = -Kx, \tag{3}$$

where $K := [k_1\ k_2\ k_3]$ is the gain vector minimizing the cost function $\int_0^\infty \left(x^\top(\tau)Qx(\tau) + Ru^2(\tau)\right)d\tau$, where the matrix $Q > 0$ and the scalar $R > 0$ are the design parameters.

Under the control law (3), the upper equilibrium of the pendulum is locally asymptotically stable with a domain of attraction depending on the design parameters. However, to implement the law (3) measurements of the velocities $\dot{\theta}$ and $\dot{\theta}_r$ are required; if these variables are not measured directly, then a velocity observer should be used to generate the estimates $\hat{\dot{\theta}}$ and $\hat{\dot{\theta}}_r$, and the law (3) takes the form

$$u = -K \left[\theta \ \hat{\dot{\theta}} \ \hat{\dot{\theta}}_r\right]^\top. \quad (4)$$

The estimates $\hat{\dot{\theta}}$, $\hat{\dot{\theta}}_r$ can be obtained with a linear Luenberger-like observer. Being widely used and rather simple in implementation, this approach is based on the linearized dynamics (2). Hence, the linear observer converges only in a neighborhood of the equilibrium and, moreover, the transient performance can significantly degrades for initial conditions being far from the origin. This drawback can be partially alleviated using linear observers with time-varying gains, *e.g.* an observer with gains scheduling, but such systems are typically harder to implement. In what follows, we propose to use nonlinear velocity observers, namely *homogeneous differentiators*, to obtain the estimates with a finite time of convergence.

3. FINITE TIME VELOCITY OBSERVER

By design, the homogeneous differentiator proposed in Perruquetti and Floquet (2007); Perruquetti et al. (2008) is applied to a chain of integrators with known input-output injections and with a scalar output signal. Thus, to use it for velocity estimation for the pendulum system considered in this paper, we apply it to each degree of freedom separately, *i.e.* we construct two observers, one for the pendulum itself, and another for the reaction wheel.

Pendulum velocity observer. From (1) we obtain the dynamics of the pendulum: $\ddot{\theta} = -\frac{k}{J}I + \frac{mlg}{J}\sin(\theta)$. Let $\hat{x}_p \in \mathbb{R}^2$ be an estimate of the vector $x_p := \left[\theta \ \dot{\theta}\right]^\top$ and define the estimation error as $e_p := \hat{x}_p - x_p$, where we recall that $e_{p,1} = \hat{\theta} - \theta$ is measured. Denote for any real numbers x and $\alpha > 0$

$$\lceil x \rfloor^\alpha := |x|^\alpha \operatorname{sgn}(x),$$

where $\operatorname{sgn}(\cdot)$ is the sign function. Following Perruquetti and Floquet (2007), we construct the homogeneous velocity observer as a differentiator of $x_{p,1}$:

$$\begin{aligned} \dot{\hat{x}}_{p,1} &= \hat{x}_{p,2} - k_{p,1}\lceil e_{p,1} \rfloor^{\alpha_p}, \\ \dot{\hat{x}}_{p,2} &= -\frac{k}{J}I + \frac{mlg}{J}\sin(\theta) - k_{p,2}\lceil e_{p,1} \rfloor^{2\alpha_p - 1}, \\ \hat{\dot{\theta}} &= \hat{x}_{p,2}, \end{aligned} \quad (5)$$

where α_p, $k_{p,1}$, $k_{p,2}$ are the design parameters. Then the error dynamics is given by

$$\begin{aligned} \dot{e}_{p,1} &= e_{p,2} - k_{p,1}\lceil e_{p,1} \rfloor^{\alpha_p}, \\ \dot{e}_{p,2} &= -k_{p,2}\lceil e_{p,1} \rfloor^{2\alpha_p - 1}. \end{aligned} \quad (6)$$

Note that $e_p = 0$ is the only equilibrium of the system (6).

Proposition 1. (Perruquetti et al. (2008)). Consider the system (6), where $\alpha_p \in \left(\frac{1}{2}, 1\right)$ and $k_{p,1}$, $k_{p,2}$ are chosen such that the polynomial $s^2 + k_{p,1}s + k_{p,2}$ is Hurwitz. Let $e_p(t)$ be the solution with the initial conditions $e_p(0) \in \mathbb{R}^2 \setminus \{0\}$. Then the origin is finite-time stable, *i.e.* there exists $T = T(e_p(0)) > 0$ such that $e_p(t)$ is defined and unique on $[0, T)$, bounded, and $\lim_{t \to T} e_p(t) = 0$. T is called the *settling-time function* of the system (6). The settling-time function can be extended at the origin by $T(0) = 0$.

The proof of Proposition 1 follows applying Theorem 10 from Perruquetti et al. (2008) to the system (6).

Reaction wheel velocity observer. For the reaction wheel dynamics we have from (1): $\ddot{\theta}_r = \frac{(J+J_r)k}{JJ_r}I - \frac{mlg}{J}\sin(\theta)$. Let $\hat{x}_r \in \mathbb{R}^2$ be an estimate of the vector $x_r := \left[\theta_r \ \dot{\theta}_r\right]^\top$ and define the estimation error as $e_r := \hat{x}_r - x_r$, where $e_{r,1}$ is measured. Similarly to (5), we construct the homogeneous velocity observer as

$$\begin{aligned} \dot{\hat{x}}_{r,1} &= \hat{x}_{r,2} - k_{r,1}\lceil e_{r,1} \rfloor^{\alpha_r}, \\ \dot{\hat{x}}_{r,2} &= \frac{(J+J_r)k}{JJ_r}I - \frac{mlg}{J}\sin(\theta) - k_{r,2}\lceil e_{r,1} \rfloor^{2\alpha_r - 1}, \\ \hat{\dot{\theta}}_r &= \hat{x}_{r,2}, \end{aligned} \quad (7)$$

where α_r, $k_{r,1}$, $k_{r,2}$ are the design parameters. Then the error dynamics is given by

$$\begin{aligned} \dot{e}_{r,1} &= e_{r,2} - k_{r,1}\lceil e_{r,1} \rfloor^{\alpha_r}, \\ \dot{e}_{r,2} &= -k_{r,2}\lceil e_{r,1} \rfloor^{2\alpha_r - 1}. \end{aligned} \quad (8)$$

The system (8) is similar to (6) and the finite-time stability of the equilibrium $e_r = 0$ follows from Proposition 1 choosing $\frac{1}{2} < \alpha_r < 1$ and $k_{r,1}$, $k_{r,2}$ such that the polynomial $s^2 + k_{r,1}s + k_{r,2}$ is Hurwitz.

Closed-loop system behavior. Given the finite-time observers, it follows that the control law (4), (5), (7) locally stabilizes the system (1). Indeed, it is known that the control law (3) that stabilizes the linearized system (2) is locally stabilizing for the nonlinear system (1). Let us denote the region of attraction under the control law (3) as Ω_α. For the observers (5) and (7) there exists a common settling time $T = T(e_p(0), e_r(0))$, which is the maximum of the settling times of these observers, and the control laws (3) and (4) are equivalent for $t \geq T$. Since the trajectories $\hat{x}_p$ and $\hat{x}_r$ are bounded, there exist constants $\bar{e}_p > 0$, $\bar{e}_r > 0$, and a set $\Omega_\beta \subset \Omega_\alpha$, such that for all initial conditions satisfying $x(0) \in \Omega_\beta$, $\|e_p(0)\| < \bar{e}_p$, $\|e_r(0)\| < \bar{e}_r$ trajectories $x(t)$ stay in Ω_α for $t \in [0, T]$. Then starting from $t = T$ we can consider the system (1) under the control law (4), (5), (7) as the system (1) under the control law (3) with the initial condition $x(T) \in \Omega_\alpha$ ensuring $x(t) \to 0$.

The set Ω_β, which is the domain of attraction under the control (4), (5), (7), depends on the design parameters and initial conditions, and is typically smaller than the set Ω_α, which is the domain of attraction under the control (3). However, given $e_p(0) = e_r(0) = 0$ we have $T = 0$ and the sets Ω_β and Ω_α coincide.

4. BEHAVIOR UNDER BIASED MEASUREMENT

The proposed control law (4), (5), (7) was successfully implemented with the experimental testbed, see Section 6 for details on the equipment. Given that the optical encoder measuring θ is perfectly adjusted, stabilization of the pendulum in the upper equilibrium and convergence $x(t) \to 0$ were achieved.

However, it was found that if the zero reading of the sensor does not coincide with the equilibrium position and the angle θ is measured with a certain constant offset, then the control goal is not achieved. This problem is well-known, see *e.g.* Block et al. (2007); Gajamohan et al. (2012). Denote the constant offset as d and let the measured signal be

$$y = \theta + d. \quad (9)$$

Using y in place of the real value θ in (3) yields $u = -K\left[y\ \dot{\theta}\ \dot{\theta}_r\right]^\top = -Kx - K\left[d\ 0\ 0\right]^\top$. Then the equilibrium of the linearized system (2) under this control law can be found as

$$x_{eq,d} = (A - BK)^{-1}BK\left[d\ 0\ 0\right]^\top = \left[0\ 0\ -d\frac{k_1}{k_3}\right]^\top.$$

It means that when measurements are biased, then the pendulum is stabilized at the upper position, however the reaction wheel does not stop and $\dot{\theta}_r$ converges to a non-zero constant value.

Consider now behavior of the velocity observers (5), (7) under biased measurements, where we impose the following assumption.

Assumption 1. The sensor offset d is sufficiently small and $\sin(d) \approx d$, $\cos(d) \approx 1$.

Using y as a measurement of θ in (5) and noting that $\hat{\theta} - y = e_{p,1} - d$, the error dynamics (6) takes the form

$$\begin{aligned} \dot{e}_{p,1} &= e_{p,2} - k_{p,1}\lceil e_{p,1} - d\rfloor^{\alpha_p}, \\ \dot{e}_{p,2} &= a_1\cos(\theta)d - k_{p,2}\lceil e_{p,1} - d\rfloor^{2\alpha_p - 1}, \end{aligned} \tag{10}$$

where we define $a_1 := \frac{mlg}{J}$. Obviously, $e_p = 0$ is not an equilibrium of this system. Considering the pendulum in the upper half-plane where $\cos(\theta) > 0$, at the equilibrium of the system (10) we have the steady-state velocity estimation error

$$e^0_{p,2} := k_{p,1}\left(\frac{a_1\cos(\theta)}{k_{p,2}}|d|\right)^{\frac{\alpha_p}{2\alpha_p - 1}}\operatorname{sgn}(d). \tag{11}$$

Analyzing the error dynamics of the reaction wheel observer, it can be shown that the steady-state velocity estimation error is $e^0_{r,2} = -e^0_{p,2}$. Applying these results to the control law (4), it follows

$$\begin{aligned} x_{eq,d} &= (A - BK)^{-1}BK\begin{bmatrix} d \\ e^0_{p,2} \\ e^0_{r,2} \end{bmatrix} \\ &= \begin{bmatrix} 0 \\ 0 \\ e^0_{p,2}\frac{k_3 - k_2}{k_3} - d\frac{k_1}{k_3} \end{bmatrix}. \end{aligned} \tag{12}$$

The conclusion is that when the measurements are biased, the velocity estimates do not converge to the real values but are biased. The pendulum stabilizes in the upper equilibrium, but the reaction wheel keeps rotating. To deal with the biased sensor we propose to construct a reduced-order bias observer, described in the following section.

Remark 1. It is worth noting that if the reaction wheel position θ_r is measured with a constant bias d_r while the pendulum position θ is measured without a distortion, then the error dynamics of the observer (7) becomes

$$\begin{aligned} \dot{e}_{r,1} &= e_{r,2} - k_{r,1}\lceil e_{r,1} - d_r\rfloor^{\alpha_r}, \\ \dot{e}_{r,2} &= -k_{r,2}\lceil e_{r,1} - d_r\rfloor^{2\alpha_r - 1}. \end{aligned}$$

It follows that at the equilibrium we have $e_{r,2} = 0$, *i.e.* a bias of the reaction wheel sensor does not lead to a steady-state bias of the estimate $\hat{x}_{r,2}$ of the reaction wheel velocity.

5. REDUCED-ORDER BIAS OBSERVER

5.1 Reduced-order observer design

Define the extended state vector $z := \left[x^\top\ d\right]^\top = \left[\theta\ \dot{\theta}\ d\right]^\top$. Then the measured signal is given by $y = [1\ 0\ 1]\,z$. Let $\hat{z}$ be an estimate of z and define $e := \hat{z} - z$. Then e_3 is the bias estimation error. Motivated by Assumption 1, we expect that the estimate of the bias is also small and the following approximation holds:

$$\sin(z_1) = \sin(y - z_3) \approx \sin(y - \hat{z}_3) + \cos(y - \hat{z}_3)e_3.$$

Then the dynamics of z can be written as

$$\begin{aligned} \dot{z} &= \begin{bmatrix} z_2 \\ -\frac{k}{J}I + a_1\sin(z_1) \\ 0 \end{bmatrix} \\ &= \begin{bmatrix} z_2 \\ a_1\cos(y - \hat{z}_3)e_3 \\ 0 \end{bmatrix} + \begin{bmatrix} 0 \\ \beta_z \\ 0 \end{bmatrix}, \end{aligned} \tag{13}$$

where the signal β_z is available, $\beta_z := -\frac{k}{J}I + a_1\sin(y - \hat{z}_3)$.

If the velocity z_2 is measured, then the reduced-order Luenberger-like linear observer of d can be constructed as

$$\begin{aligned} \dot{v} &= \beta_z, \\ \hat{z}_3 &= L(v - z_2), \\ \hat{d} &= \hat{z}_3, \end{aligned} \tag{14}$$

where L is the design parameter. Then

$$\dot{e}_3 = -La_1\cos(y - \hat{z}_3)e_3. \tag{15}$$

As we consider the pendulum around the upper equilibrium, it is reasonable to impose the following assumption.

Assumption 2. For trajectories of the system there exists [1] $c_0 > 0$ such that $\min\left(\cos(y - \hat{d}), \cos(\theta)\right) > c_0$ along these trajectories.

Under this Assumption, it is obvious that choosing $L > 0$ in (15) yields to exponential convergence of e_3 to zero. With the estimator (14), the stabilizing control law (4) can be rewritten as

$$u = -K\left[y - \hat{d}\ \hat{\dot{\theta}}\ \hat{\dot{\theta}}_r\right]^\top. \tag{16}$$

5.2 Closed-loop convergence

Let us now consider what happens when the reduced-order bias observer is in the loop with the homogeneous velocity observer. In such a case the state z_2 in the observer (14) is not measured directly but generated by the observer (5). At the same time, the estimate $\hat{z}_3$ is used to compensate the bias and we substitute $y - \hat{z}_3$ in place of θ in (5). The joint observers dynamics is now given by

$$\begin{aligned} \dot{\hat{z}}_1 =& \hat{z}_2 - k_{p,1}\lceil \hat{z}_1 + \hat{z}_3 - y\rfloor^{\alpha_p}, \\ \dot{\hat{z}}_2 =& -\frac{k}{J}I + a_1\sin(y - \hat{z}_3) \\ & - k_{p,2}\lceil \hat{z}_1 + \hat{z}_3 - y\rfloor^{2\alpha_p - 1}, \\ \dot{v} =& -\frac{k}{J}I + a_1\sin(y - \hat{z}_3), \\ \hat{z}_3 =& L(v - \hat{z}_2). \end{aligned} \tag{17}$$

[1] In practical applications this assumption can be ensured restricting, *e.g.* by a projection operator, possible variations of $\hat{z}_3$ subject to known bounds of the displacement d.

To proceed with the dynamics analysis note that $\hat{z}_1 + \hat{z}_3 - y = e_1 + e_3$ and that under the imposed assumptions the following approximation holds: $\sin(y - \hat{z}_3) = \sin(z_1 - e_3) \approx \sin(z_1) - \cos(z_1)e_3$. Denote $s := [e_1 + e_3 \;\; e_2 \;\; e_3]^\top$. Then the error dynamics of the observer yields

$$\begin{aligned}\dot{s}_1 &= s_2 - k_{p,1}\lceil s_1 \rfloor^{\alpha_p} + Lk_{p,2}\lceil s_1 \rfloor^{2\alpha_p - 1},\\ \dot{s}_2 &= -a_1\cos(z_1)s_3 - k_{p,2}\lceil s_1 \rfloor^{2\alpha_p - 1},\\ \dot{s}_3 &= Lk_{p,2}\lceil s_1 \rfloor^{2\alpha_p - 1}.\end{aligned} \tag{18}$$

Since $\cos(z_1) > c_0$, the only equilibrium of (18) is the origin $s = e = 0$. However, the error dynamics (18) is not homogeneous for $\alpha_p < 1$ and thus it does not have the finite-time stability property. An important observation is that for $\alpha_p = 1$ the system (18) becomes a linear time-varying (due to $\cos(z_1)$) system. The following proposition establishes convergence of the extended observer for α_p in a vicinity of 1.

Proposition 2. Consider the observer (17) for the system (13) under Assumption 2 with the error dynamics (18). Define

$$A_m := \begin{bmatrix} -k_{p,1} + Lk_{p,2} & 1 & 0 \\ -k_{p,2} & 0 & -a_1c_0 \\ Lk_{p,2} & 0 & 0 \end{bmatrix},$$

$$A_M := \begin{bmatrix} -k_{p,1} + Lk_{p,2} & 1 & 0 \\ -k_{p,2} & 0 & -a_1 \\ Lk_{p,2} & 0 & 0 \end{bmatrix},$$

and

$$A_1 := \begin{bmatrix} Lk_{p,2} - \frac{1}{2}k_{p,1} & 0 & 0 \\ -k_{p,2} & 0 & 0 \\ Lk_{p,2} & 0 & 0 \end{bmatrix},$$

where c_0 is defined in Assumption 2. If the parameters of the observer (17) are chosen such that the there exists a positive-definite symetric matrix P satisfying the LMIs

$$\begin{aligned} PA_m + A_m^\top P + \gamma P &\le 0,\\ PA_M + A_M^\top P + \gamma P &\le 0,\\ PA_1 + A_1^\top P &\le 0,\end{aligned} \tag{19}$$

for some $\gamma > 0$, then there exist $\varepsilon_\alpha > 0$ and a compact set Ω_α, such that for $\alpha \in (1 - \varepsilon_\alpha, 1]$ and all initial conditions $s(0) \in \Omega_\alpha$ it holds $s \to 0$ and $\lim_{t\to\infty} |\hat{z} - z| = 0$.

The proof of the proposition is omitted due to the lack of space.

Remark 2. The LMIs (19) are used to check if the given set of gains $k_{p,1}$, $k_{p,2}$, and L is stabilizing. Using standard LMIs arguments, see Boyd et al. (1994), this feasibility check can be reformulated in order to find (if any) such gains, that (19) are feasible.

Estimation of the domain of attraction Ω. Suppose we are given P being a solution of (19) for some c_0 and γ and Δ_M being the maximum value Δ_α. First, compute Q and find λ_Q as the smallest generalized eigenvalue of γP and Q, *i.e.* the smallest value such that $\det(\gamma P - \lambda_Q Q) = 0$. Then $\dot{V}$ is negative definite if $\ln(s_1^2)\,\Delta_\alpha < \lambda_Q$. Next, compute s_M as $s_M = \exp\left(\frac{\lambda_Q}{\Delta_M}\right)$. To estimate Ω we have to find such C that $s^\top P s < C \Rightarrow s_1^2 < s_M$, *i.e.* we are looking for the ellipsoid $s^\top P s = C$ that touches the plane $s_1 = \sqrt{s_M}$. Since P is positive definite, there exists matrix $R = R^\top$ such that $P = RR$. Then $s^\top P s = v^\top v$ where the new coordinates are $v = Rs$. Now $s^\top P s = C$ is a sphere $v^\top v = C$ with the radius $\sqrt{C}$ in the new coordinates. The plane $s_1 = \sqrt{s_M}$ in the s coordinates is defined by the normal vector $n_s := [1 \; 0 \; 0]^\top$ and the point $p_s = [\sqrt{s_M} \; 0 \; 0]^\top$. In the v coordinates we have the point $p_v = Rp_s$ and the normal vector $n_v = R^{-1}n_s$. Then the distance from the plane in v coordinates to the origin is given by $\sqrt{C} = \frac{n_v^\top p_v}{|n_v|} = \sqrt{\frac{s_M}{n_s^\top R^{-2} n_s}}$, hence $C = \frac{s_M}{(P^{-1})_{1,1}}$, where $\left(P^{-1}\right)_{1,1}$ is the $(1,1)$ element of the matrix P^{-1}.

Remark 3. It is worth noting that the set Ω is obviously a conservative estimate of the real domain of attraction.

Table 2. Controller parameters used in experiments.

Description	Symbol	Value
LQR gains in (4) and (16)	K	$\begin{bmatrix}-581.6 & -83.4 & -1.2\end{bmatrix}$
Parameters in (5)	$[k_{p,1}, k_{p,2}, \alpha_p]$	[7, 12, 0.75]
Parameters in (7)	$[k_{r,1}, k_{r,2}, \alpha_r]$	[7, 12, 0.75]
Gain of the bias observer (14)	L	0.033

6. EXPERIMENTS

The hardware for the tests (shown in Figure 1) is assembled from off-the-shelf components. The reaction wheel (a bicycle brake rotor) is driven by a 70W Maxon EC 45 flat brushless DC motor, which is controlled using Maxon EPOS2 50/5 in torque mode. A STM32F407 discovery board was chosen as the main computing unit.

For our experiments, we consider the problem of the upright pendulum stabilization, where the initial position is in a neighborhood of the equilibrium. We use the homogeneous velocity observers (5) and (7) with the feedback control law (4). At it is mentioned in Section 4, if the optical encoder is perfectly adjusted and $d = 0$ in (9), then the proposed controller achieves the goal and stabilizes the pendulum. In what follows we consider the problem of stabilization under biased measurements, where the sensor offset d in (9) is $d \approx 5^\circ \approx 0.09$. Table 2 lists the parameters used in the experiments.

First, we illustrate that the same control law (4), (5), and (7) cannot stabilize the pendulum for $d \neq 0$. As it is shown in (12), the pendulum arrives to the upper position, but the reaction wheel does not stop and maintains a nonzero constant velocity. The experimental results are depicted in Figure 2. Here the measured angle y converges to a nonzero value, such that $y \approx d$, and the physical angle $\theta \approx 0$. Velocity estimates $\hat{x}_{p,2}$ and $\hat{x}_{r,2}$ converge to nonzero values, where the estimation errors are predicted by (11). The physical velocities converge to $\dot{\theta} \approx 0$ and $\dot{\theta}_r \approx 156$ radians per second, that corresponds to (12).

Next we apply the approach by Gajamohan et al. (2012). The key observation of this approach is that under the control law (4) the pendulum angle θ reaches zero, and is steady state it holds $y \approx d$. Thus, the measurement y can be used as an estimate $\hat{d}$, which is then injected in (16). To avoid stability issues, estimation of d is performed in a slower time scale than stabilization that is ensured by a low-pass linear filter:

$$\tau_d \frac{d}{dt}\hat{d}(t) + \hat{d}(t) = y(t), \tag{20}$$

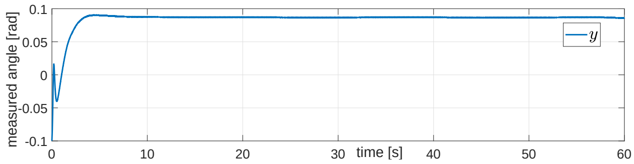

(a) Angle measurement

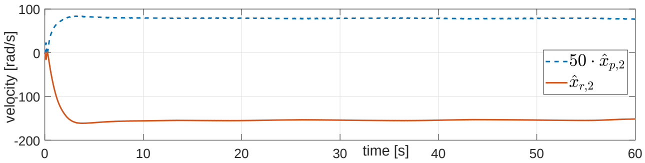

(b) Velocity estimates

Fig. 2. The control law (4), (5), and (7) for $d \approx 0.09$.

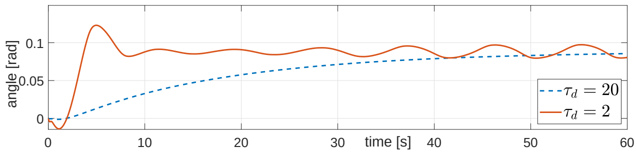

(a) Bias estimate $\hat{d}$

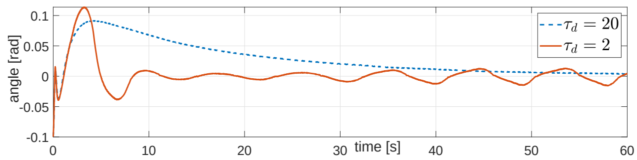

(b) Estimate of the pendulum position $\hat{\theta} = y - \hat{d}$

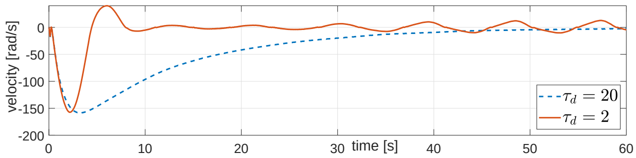

(c) Velocity estimate $\hat{x}_{r,2}$

Fig. 3. The control (5), (7), (16), and (20) for $d \approx 0.09$. For $\tau_d = 20$ the system is stabilized in approx. 60 seconds. For $\tau_d = 2$ transients are faster but closed-loop oscillations appear.

where $\tau_d > 0$. The drawback of this approach is that if τ_d is large enough, then the stabilization goal is achieved but with a long transient time. If the value τ_d is reduced to accelerate the transients, then the closed-loop stability can be compromised. Results of the experiments with the velocity observers (5), (7), bias observer (20), and control law (16) are depicted in Figure 3 for $\tau_d = 20$ and $\tau_d = 2$ and illustrate the trade-off between the transient time and the closed-loop stability.

Finally, we perform an experiment with the reduced-order bias observer (14). Results of the experiment are shown in Figure 4 and illustrate stabilization of the pendulum with fast transients.

7. CONCLUSION

The problem of velocity observer design for an inverted reaction-wheel pendulum under biased measurements was considered in the paper. The proposed solution combines a HOMD-based velocity observer with a reduced-order bias estimator. It is shown that the stability of the proposed observer is ensured under a proper choice of tuning parameters. Experimental results illustrate the performance of the proposed approach.

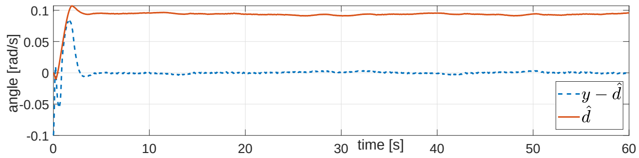

(a) Bias estimate $\hat{d}$ and estimate of the pendulum position $\hat{\theta} = y - \hat{d}$

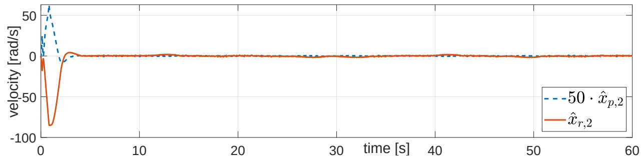

(b) Velocity estimates

Fig. 4. The control (5), (7), and (16) with the reduced order observer (14) for $d \approx 0.09$.

As a further research direction, we consider robustness analysis for time-varying parameters and model uncertainties and application of the proposed nonlinear observer for walking robot stabilization, see Ryadchikov et al., 2018.

REFERENCES

Aranovskiy, S., Ortega, R., Romero, J.G., and Sokolov, D. (2017). A globally exponentially stable speed observer for a class of mechanical systems: experimental and simulation comparison with high-gain and sliding mode designs. *International Journal of Control*, 0(0), 1–14.

Block, D.J., Åström, K.J., and Spong, M.W. (2007). The reaction wheel pendulum. *Synthesis Lectures on Control and mechatronics*, 1(1), 1–105.

Boyd, S., El Ghaoui, L., Feron, E., and Balakrishnan, V. (1994). *Linear matrix inequalities in system and control theory*, volume 15. Siam.

Gajamohan, M., Merz, M., Thommen, I., and D'Andrea, R. (2012). The cubli: A cube that can jump up and balance. In *2012 IEEE/RSJ International Conference on Intelligent Robots and Systems*, 3722–3727.

Levant, A. (1998). Robust exact differentiation via sliding mode technique. *Automatica*, 34(3), 379–384.

Perruquetti, W. and Floquet, T. (2007). Homogeneous finite time observer for nonlinear systems with linearizable error dynamics. In *2007 46th IEEE Conference on Decision and Control*, 390–395.

Perruquetti, W., Floquet, T., and Moulay, E. (2008). Finite-time observers: Application to secure communication. *IEEE Transactions on Automatic Control*, 53(1).

Ryadchikov, I., Sechenev, S., Drobotenko, M., Svidlov, A., Volkodav, P., Vishnyakov, R., Sokolov, D., and Nikulchev, E. (2018). Stabilization system of a bipedal non-anthropomorphic robot anywalker. *Journal of Engineering Science and Technology Review*, 11, 128–133.

Spong, M.W., Corke, P., and Lozano, R. (2001). Nonlinear control of the reaction wheel pendulum. *Automatica*, 37(11), 1845 – 1851.

Vasiljevic, L.K. and Khalil, H.K. (2008). Error bounds in differentiation of noisy signals by high-gain observers. *Systems & Control Letters*, 57(10), 856–862.